Optimising the performance of optical data storage drives based on a novel seesaw–swivel actuator for a holographic module

Yu-Cheng Lin[1], Po-Chien Chou[1], Kuan-Chou Hou[2], Stone Cheng[2], Jin-Chern Chiou[3], Hsi-Fu Shih[4]

[1]*Department of Mechanical Engineering, National Chiao Tung University, Hsinchu 30010, Taiwan*
[2]*Institution of Electrical and Control Engineering, National Chiao Tung University, Hsinch 30010, Taiwan*
[3]*School of Medicine, China Medical University, Taichung 40402, Taiwan*
[4]*Mechanical Engineering Department, National Chung-Hsing University, Taichung 402, Taiwan*
E-mail: owan0518@hotmail.com

Published in Micro & Nano Letters; Received on 14th March 2011; Revised on 11th July 2011

This Letter presents an optical module with a holographic optical element (HOE) for the small-form-factor pickup head. The proposed module is mounted on a novel seesaw swivel-drive mechanism with unique features, including a rotary actuator for track-following; in addition, a seesaw arm nutates along a pivot for laser focusing. Additionally, the actuating force is increased within the limit of actuator size constraints by using a Halbach-magnet-array in biaxial voice coil motors. Experimental assessment of the holographic module and actuator reveals that the HOE module ensures the optical performance and stability of the system, together with a performance superior to a classic hinge-type swing arm actuator, as attributed to enhanced durability and higher robustness.

1. Introduction: This work describes an innovative optical configuration with a holographic optical element (HOE) for small-form-factor (SFF) pickup design, as developed to comply the requirements of new generation of optical devices [1–3]. The overall module of the optical system is then mounted on the seesaw–swivel actuator to perform the laser focusing and track-following operations. Next, the dynamic characteristics of electromagnetic and structural analyses are studied by deriving this biaxial actuator design. Additionally, an attempt is made to reduce the thickness of driving mechanism without sacrificing the actuating force by utilising the proposed ring yoke with Halbach-magnet-array (HMA) to the increase magnetic flux of one side without the cover yoke. All structural and electromagnetic circuit parts are optimised in numerical simulations to evaluate the biaxial motion performance. Furthermore, the optimised design that satisfies all specifications is explained [4, 5]. Finally, the stability and performance of the proposed holographic module and actuator are evaluated [6, 7].

2. Device design: SFF optical configuration design by using an HOE is based on the optical specifications in Fig. 1. The proposed devices are fabricated and tested to demonstrate the uniqueness of their performances and advantages over conventional ones. After the 45° turning mirror (not shown) reflects the horizontal laser beam upwards, microprisms 2 and 1 redirect the beam upwards towards HOE. After the reflected beam enters HOE perpendicularly, the zero-order laser beam passes through the objective lens and focuses on the optical disk. In this work, HOE is developed as a beam-splitting element to simplify the optical path and optical components. In the optical return path, the returning beam is diffracted by the HOE patterns and reflected by microprism 1 to microprism 2. The microprisms provide support substrates as well as calibration reference planes based on the virtual image method. Finally, the returning beam projected on the quadrant photodetector (PD) generates the focus error signal (FES), tracking error signal (TES) and radio frequency signal (RFS) from the HOE diffraction.

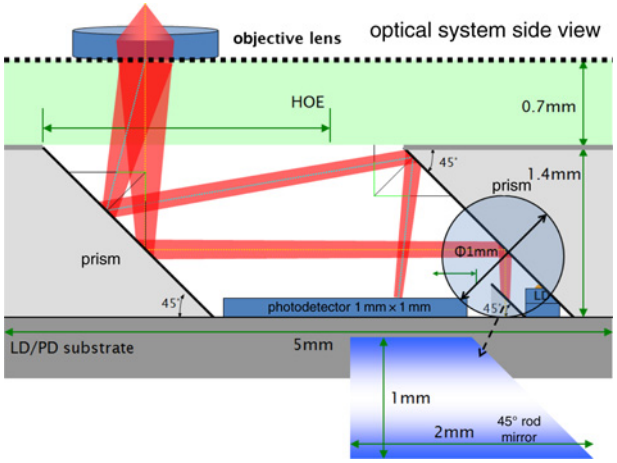

Figure 1 *Schematic diagram of the optical head, where the laser is bounded on a submount and emitting light from the direction into the paper*

The assembly process of this HOE module optical head are illustrated in Fig. 2. This device is fabricated and tested to achieve the microminiaturisation of optical sensor. The 635 nm laser assembly technology is utilised to play an important role in stabilising new holographic pickup structures. In Fig. 2*a*, 635 nm edge-emitting laser diode chip, a quadrant photodetector and a 45° turning mirror are mounted on a substrate. Fig. 2*b* showed two microprisms are stuck on two sides of the substrate. In Fig. 2*c*, an HOE module is bound on these two prisms. In the final step, Fig. 2*d*, an objective lens module (objective lens and lens holder) is adjusted on HOE via astigmatic focus detection method.

Many previous works use the swing arm type to realise the microstorage system [8, 9]. An effective solution increases the second torsion mode to limit the servo bandwidth of the actuating range, whereas the other one strengthens the hinge connection with embossments to optimise the suspension shape; the excessive load between the suspension and swing arm also diminishes the mechanical durability. However, the hinge springs are susceptible to permanent fracturing under long-term operating conditions. Consequently, the durability of the actuator is improved by designing a seesaw-type rotary actuator without a hinge spring to provide the miniaturisation and enable the nutation to focus on the motion. Fig. 3 shows the overall structure of the seesaw actuator. The composite alloy seesaw arm is connected to two steel balls by the fixed cylinder pins. The cylinder pin restricts the ball, which makes contact with the side of arm and provides one degree of freedom in vertical axis (with the direction of the pin clamped). Between the seesaw arm and the pins is a rotary junction, which consists of a lateral bracket. The function of a limited working distance (±0.2 mm) that is less than the effective focal length (0.525 mm) can avoid abrupt impacts on the head to damage the disk.

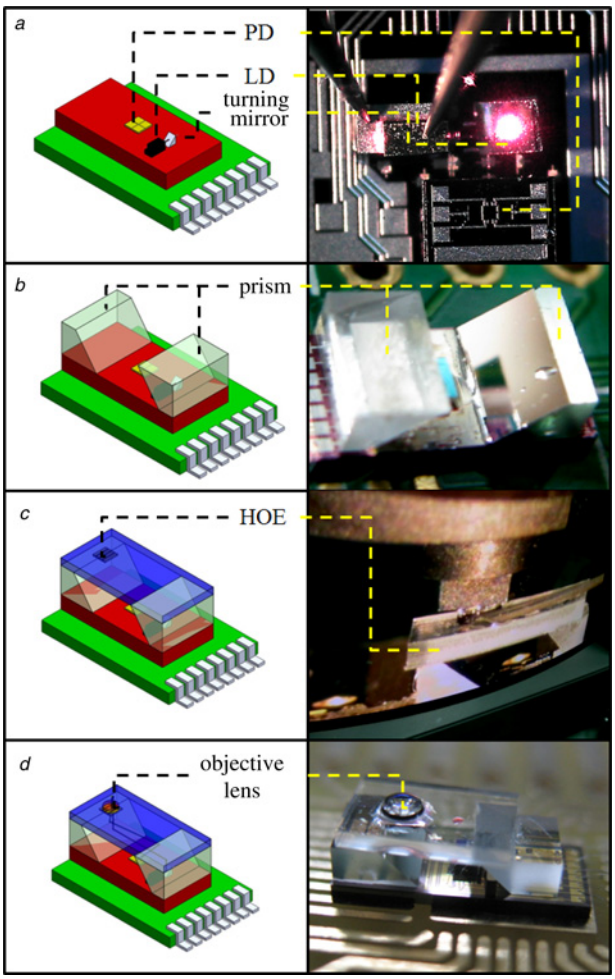

Figure 2 *Fabrication processes of the HOE module sensor*
a Laser diode, photodiode and turning mirror
b 45° prisms
c HOE glass substrate
d Objective lens modulus

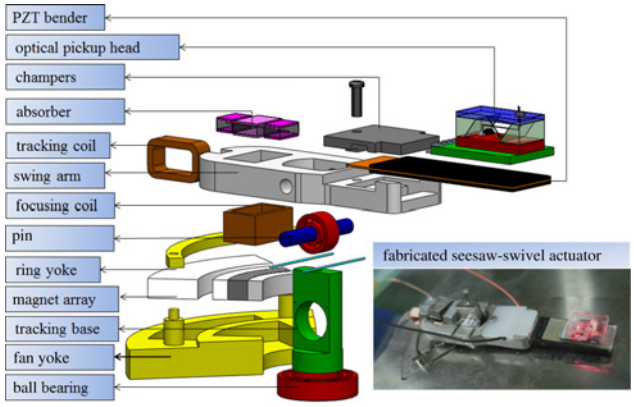

Figure 3 *Structure of the seesaw–swivel actuator for SFF pickup head*

Moreover, this study uses the HMA array to achieve vertical focusing motion, despite its potential for tracking actuator usage [10]. The ring yoke with HMA has a thin actuation structure without sacrificing flux density. Owing to its unique magnet array feature that increases the magnetic flux on one side without using a cover yoke, each dimension of the array is obtained to achieve higher actuation performance, optical path and optical components. In the optical return path, the returning beam is diffracted by the HOE patterns and reflected by microprism 1 to microprism 2. The microprisms provide support substrates as well as calibration reference planes based on the virtual image method. Finally, the returning beam projected on the quadrant PD generates the FES, TES and RFS from the HOE diffraction.

3. Performance evaluation and optimisation: The design process of a seesaw arm is optimised for the seesaw-type actuator to comply with actuation performance requirements. The dynamic characteristics, that is modal shapes, of the seesaw arm-type actuator are analysed using finite-element methods. Fig. 4 illustrates the finite-element meshes and mode analysis. For the simulation, Table 1 lists the resonance frequencies of various vibrational modes.

Driving mechanism is optimised to determine the size constraints without hindering the performance by the voice coil motor (VCM) actuation force. Fig. 5 shows this optimisation, which starts by defining six varied dimensions of the structural parts as design variable candidates and also, determining their corresponding constraints that arise from the limited space. The optimal sizing

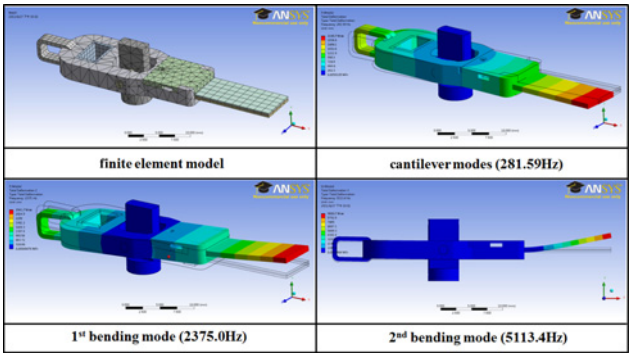

Figure 4 *Finite-element model and vibrational modes*

Table 1 Tolerance and optima value of six design parameters

Paremeters	A	B	C	D	E	F
Initial values, X_0, mm	11	12	13	2.8	0.8	7.5
Upper bound (−10%)	9.9	10.8	11.7	2.52	0.72	6.25
Lower bound (+10%)	12.1	13.2	14.3	3.08	0.88	8.35
Optimal values	**11.2**	**13.0**	**14.1**	**3.01**	**0.85**	**8.12**

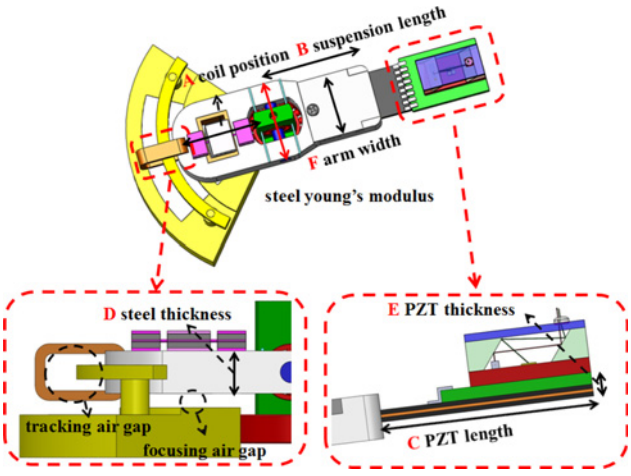

Figure 5 *Candidate six design parameters for operating optimisation*

doi: 10.1049/mnl.2011.0135

involves assigning the actuator sensitivity to maximise the objective function, with the intention of increasing the frequencies of flexible modes. Equation (1) shows the objective function. Notably, the weighting factor is not applied

$$\max\left[(F_{\text{focusing}}/F_{\text{i.focusing}})^2 + (F_{\text{tracking}}/F_{\text{i.tracking}})^2\right] \quad (1)$$

where F_{focusing} denotes the mode I in the focusing direction, and F_{tracking} refers to the mode II in the tracking direction. Additionally, $F_{\text{i.focusing}}$ and $F_{\text{i.tracking}}$ represent the initial resonance frequency, respectively. In Table 2, the optimal results are calculated within the variation of the model parameters A–F with respect to the initial model parameters A_0–F_0, in the range of, −10 to 10%, respectively.

Fig. 6 summarises the FEM analysis results for the optimised magnetic array dimensions. Based on the electromagnetic analysis, flux density and actuation force are compared with those of the cover yoke with a conventional magnet array. The important position of the magnetic flux is 0.5 mm above the magnet array surface where coils are located. Fig. 7 shows a cross-sectional magnetic flux along the A–A′ working path of the magnet array. The maximum flux density is ~0.45 T. Figs. 6 and 7 also present the flux density along the radius direction (R) with various track-following angles (θ). The flux densities are uniformly distributed on both focusing and tracking coils actuation range. A ring yoke with HMA is the optimum candidate for the seesaw–swivel actuator, capable of providing an additional 4.5% actuation force and superior thickness and mass properties over that of the ring yoke combined with the cover yoke.

4. Experimental results: Fig. 3 shows a prototype of the fabricated seesaw–swivel actuator with SFF optical head. In the experimental implementation, the relative displacement of the fabricated actuator is assessed using a laser doppler vibrometer. In addition to recording both the input and output signals of time-domain responses, a dynamic signal analyser obtains the frequency responses of the VCM actuator. Fig. 8 shows the measured frequency response of the prototype. The small resonance peak at 3.85 kHz is the first

Table 2 Characteristics of resonance frequency modes

Mode	Resonance frequency, Hz	Response
I	281.59	cantilever
II	2375.0	1st bending
III	5113.4	2nd bending

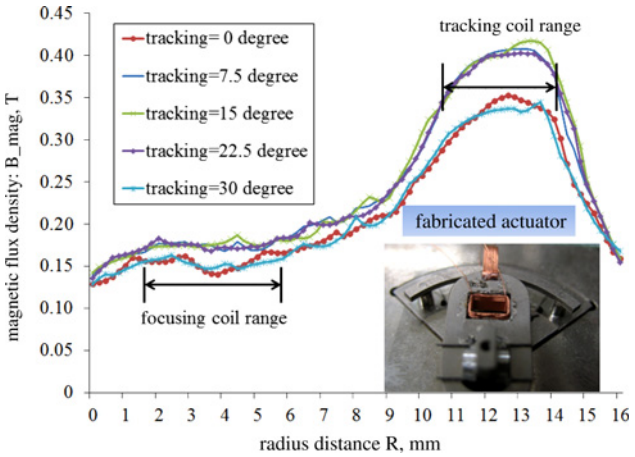

Figure 6 *3D electromagnetic analysis and air gap flux density optimisation*

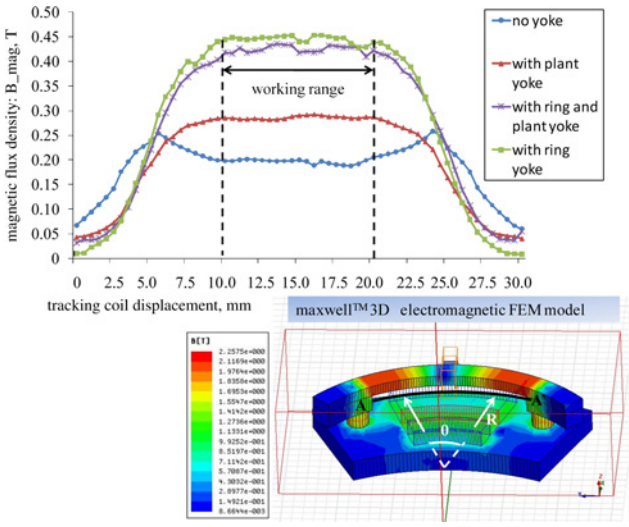

Figure 7 *FEM results from various magnetic flux variations along A–A′ polyline*

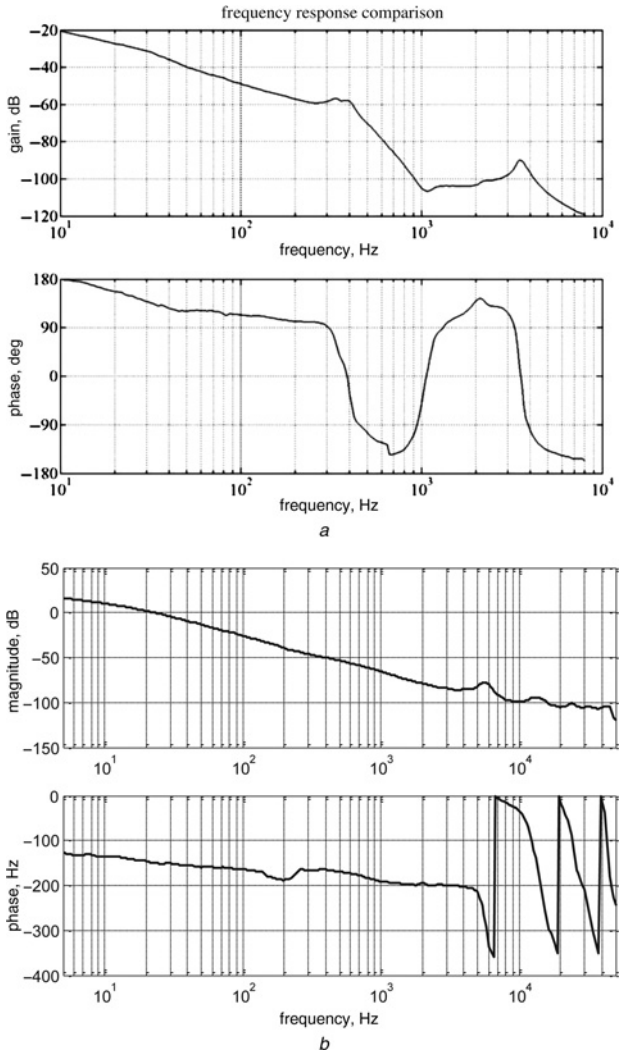

Figure 8 *Frequency responses of the fabricated seesaw–swivel device*
a Focusing direction
b Tracking direction

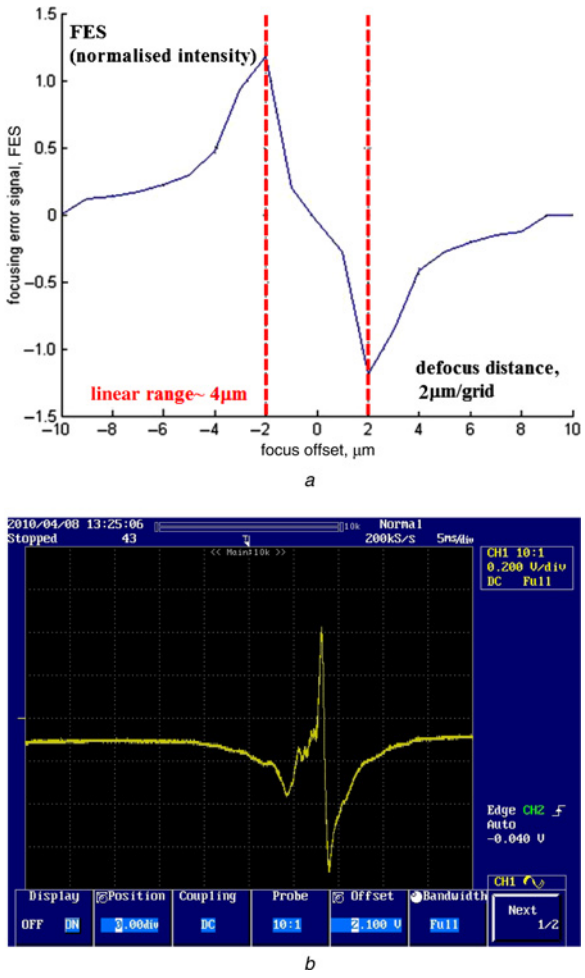

Figure 9 *Focusing error signal (S-curve)*
a Simulation
b Experimental results

bending mode of the actuator. Simulation results (4 kHz) and measurement results (3.85 kHz) slightly differ in actuation performance, possibly owing to structural differences during manufacturing and assembly. Additionally, mechanical properties identified during the experiment may also distort the results.

The experimental setup to evaluate the optical performance of the integrated SFF optical device includes an integrated SFF pickup unit, a seesaw–swivel device, an optical signal conversion amplifier and an optical disc. The quadrant detector adopts the astigmatic method for focusing detection and push–pull method for tracking detection. Additionally, an attempt is made to verify the focusing performance of this HOE optical module. To do so, the focusing actuator is driven by a 5 Hz triangular signal with a magnitude of ± 140 mV to force the optical module to pass its focal point to the disc. Fig. 8 shows the detected results, whereas the simulated symmetric *S*-curve is used for comparison. The simulation and experimental results are satisfactory and demonstrate the feasibility of the seesaw–swivel actuator with the SFF optical head (see Fig. 9).

5. Conclusions: This work has developed a novel holographic module and seesaw–swivel device design for an integrated micro pickup head for small-form-factor applications. In addition to magnifying the focusing force, this accurate level mechanism strengthens the stiffness of the load suspension. Moreover, exactly how the driving force affects this actuator is studied to elucidate the biaxial performance. Furthermore, the mechanical and electromagnetic properties are optimised to determine the size constraints without inhibiting the performance by the VCM actuation force. Also, the fabricated device is evaluated based on dynamic experiments and optical measurements. The actuator performance and the focus performance for SFF optical head are verified as well. Importantly, this work demonstrates the feasibility of this novel SFF pickup head with a seesaw–swivel device for next-generation optical storage-systems.

6. Acknowledgments: Yu-Cheng Li and Po-Chieu Chou contributed equally to this work.

7 References

[1] Shih H.F., Chang C.L., Lee K.J., Chang C.S.: 'Design of optical head with holographic optical element for small form factor drive systems', *IEEE Trans. Mag.*, 2005, **41**, pp. 1058–1060
[2] Chiu Y., Shih H.F., Chiou J.C., *ET AL.*: 'Design and fabrication of a small-form-factor optical pickup head', *IEEE Trans. Mag.*, 2009, **45**, pp. 2194–2197
[3] Yoon S.J., Lee J., Park Y.P., Choi D.H.: 'Design of optical flying Head for magnetooptical recording', *IEEE Trans. Mag.*, 2005, **41**, pp. 2851–2853
[4] Chiu C.W., Chao Paul C.P., Kao Nicholas Y.-Y., Young F.K.: 'Optimal design and experimental verification of a magnetically actuated optical image stabilization system for cameras in mobile phones', *J. Appl. Phys.*, 2008, **103**, article id 07F136
[5] He Z., Ong E.H., Guo G.: 'Optimization of a magnetic disk drive actuator with small skew actuation', *J. Appl. Phys.*, 2002, **91**, pp. 8709–8711
[6] Yu H.C., Liu T.S.: 'Adaptive model-following control for slim voice coil motor type optical image stabilization actuator', *J. Appl. Phys.*, 2008, **103**, article id 07F114
[7] Chao Paul C.P., Chiu C.W., Liang H.K., Kao Nicholas Y.Y.: 'Intelligent actuation strategy via image feedbacks for a magnetically actuated autofocusing module in mobile phones', *J. Appl. Phys.*, 2008, **103**, article id 07F123
[8] Blankenbeckler D.L., Bell B.W., Ramadurai Jr K., Mahajani R.L.: 'Recent advancements in dataplay's small form-factor optical disc and drive', *Jpn. J. Appl. Phys.*, 2006, **45**, pp. 1181–1186
[9] Lee D.J., Park S.J., Oh J., Park N.C., Park Y.P., Jung H.S.: 'Development of rotary-type voice coil motor actuator for small-form-factor optical disk drive', *Jpn. J. Appl. Phys.*, 2006, **45**, pp. 1124–1128
[10] Jeong J., Lee M.G., Lee J.H., Yoon H.K., Gweon D.G.: 'Multisegmented magnet array on voice coil motor in rotating data storage devices', *Jpn. J. Appl. Phys.*, 2004, **43**, pp. 1398–1402

doi: 10.1049/mnl.2011.0135